Journal of Advanced Research 31 (2021) 87–96

Contents lists available at ScienceDirect

Journal of Advanced Research

journal homepage: www.elsevier.com/locate/jare

Preparation of biological sustained-release nanocapsules and explore on algae-killing properties

Jinyun Li [a,b,1], Ming Guo [a,b,1,*], Yiping Wang [c], Bihuan Ye [d], Youwu Chen [d], Xuejuan Yang [b]

[a] College of Engineering, Zhejiang A&F University, Hangzhou, Zhejiang 311300, China
[b] College of Science, Zhejiang A&F University, Hangzhou, Zhejiang 311300, China
[c] College of Forestry and Bio-technology, Zhejiang A&F University, Hangzhou, Zhejiang 311300, China
[d] Zhejiang Academy of Forestry, Hangzhou, Zhejiang 310023, China

GRAPHICAL ABSTRACT

The novel bio-based sustained-release nanocapsules was prepared by microcapsule technology. Comprehensive characterization and analysis were carried out to measure the sustained release and algae-killing properties of the new nanocapsules.*Introduction:*

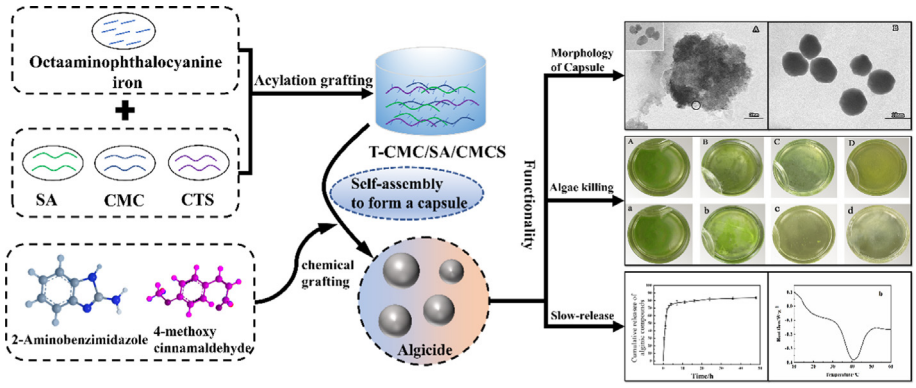

ARTICLE INFO

Article history:
Received 6 April 2020
Revised 8 December 2020
Accepted 10 December 2020
Available online 15 December 2020

Keywords:
Amphiphilic polysaccharides
Algae-killing compound
Sustained-release nanocapsules
Algae-killing performance

ABSTRACT

Introduction: Green algae seriously affect the quality and yield of Torreya grandis, it is important to explore new, environmentally friendly ways to control it.
Objectives: The present study aimed at preparing sustained-release algae-killing nanocapsules without pollution to the environment.
Methods: In this work, sodium carboxymethylcellulose (CMC), sodium alginate (SA), and chitosan (CTS) were used as raw materials in acylation reaction with the photosensitive catalytic material iron octaaminophthalocyanine (T) to generate the photoactive bio-based materials T-CMC, T-SA, and T-CMCS. Cinnamaldehyde and 2-aminobenzimidazole were combined using chemical grafting to produce a new algicide, and then formed nanocapsules by phase separation. The molecular structure of products was characterized by UV–Vis, FTIR, and NMR (^{1}H NMR, ^{13}C NMR). The particle size of the nanocapsules was determined by Zeta particle size analysis and TEM; DSC was used to investigate the thermal stability;

Peer review under responsibility of Cairo University.
* Corresponding author at: College of Engineering, Zhejiang A&F University, Hangzhou, Zhejiang 311300, China.
E-mail address: guoming@zafu.edu.cn (M. Guo).
[1] The authors contribute equally in this work.

https://doi.org/10.1016/j.jare.2020.12.006

The encapsulation efficiency and sustained-release performance were determined by HPLC. Then the phytotoxic of the new algicide was measured.
Results: The bio-based nanocapsules was successfully synthesized, which had a particle size of 10–30 nm and was stable at 40 °C. The encapsulation efficiency of the nanocapsules was 48.77%, the cumulative release rate was 83%, and the new algicide killed the green algae in a dose-dependent way.
Conclusions: The bio-based nano capsule is a new and valuable Sustained-release capsule, which is the method of green algae.

Introduction

Torreya grandis is a popular dried fruit that is valuable as a food and medicine [1]. However, due to the increasingly extreme climate and the decreases in resistance to diseases and pests, the frequency of pest outbreaks in *T. grandis* have increased year by year. Among these diseases, green algae cause the most harm to *T. grandis*. Currently the most common treatment for green algae is using stone sulfur mixtures, but this method has a low utilization rate and short validity period and cause serious environmental pollution. Thus, it must find new ways that are environmentally friendly and safe to control the green algae of *T. grandis*. In related work, the use of nanocapsules to control pesticide release has attracted extensive attention, as it can not only improve the use rate of pesticides, but can also reduce its instantaneous toxicity during application and prolong its validity period [2]. The studies on the prevention and control of *T. grandis* diseases are previously reported, but there are few reports on sustained-release pesticide capsules that can kill *T. grandis* algae. Thus, developing such a method would find useful applications.

Sustained-release pesticide capsules are commonly prepared using interfacial polymerization [3] and in-situ polymerization [4], Wang et al. [5] used hydrophobic polyacid chloride and hydrophilic polyamine in an immiscible phase in which rapid polymerization of the interface is used to prepare polyamide pH-sensitive microcapsules. Many studies have found that capsule size affects the properties of sustained-release capsules. For example, Zuo et al. [6] prepared nanocapsules using in-situ polymerization, with polypyrrole and glycerol as shell materials and ammonium persulfate as a core material. Because sustained-release pesticide nanocapsules show a unique nanosize effect, it has good biocompatibility, targeting, and sustained release [7], therefore it is important to study sustained-release pesticide nanocapsules as new agents for *T. grandis*.

The walls of such nanocapsules influence their release properties. In recent years, these materials have typically been made of high-molecular-weight polymers [8–10]. Although these capsules have good toughness and long sustained release, they are difficult to degrade and can cause secondary pollution to the environment [11]. Thus, it is important to explore new, environmentally friendly materials, such as embedding pesticides in biodegradable carriers. For example, glycosyl polymers, such as chitosan [12], alginate [13,14], and starch [15], have attracted interest because of their good biocompatibility and biodegradability [16]. Such materials can be used as sustained-release capsule walls, overcome the shortcomings of traditional materials. However, polysaccharides contain significant amounts of hydrophilic groups. These groups must be hydrophobically modified to form amphiphilic-derived polysaccharides [17–19], which then self-assemble in solvent to form a core–shell micellar structure [20,21]. When loaded with hydrophobic pesticides, such a structure can control the release of the pesticides [22], which solved the low use rate, short expiration date, and environmental pollution of chemical pesticides. Thus, preparing a new nanocapsule for killing algae will greatly benefit forestry and economics.

In this work, sodium carboxymethyl cellulose (CMC), sodium alginate (SA), and chitosan (CTS) were used for acylation reaction with the photosensitive catalytic material, iron octadaminphthalocyanine, to generate a new biological matrix. The iron octadaminphthalocyanine contained phthalocyanine (PC), a synthetic derivative of porphyrins that are non-polluting to the environment. It has good absorption in visible region and can be used as photosensitive catalyst [23]; Through chemical grafting reaction cinnamaldehyde and 2-aminobenzimidazole are combined to obtain an environmentally friendly algae killer. Using this algae-killing compound as the core, the bio-based sustained-release nanocapsule was created, with a dual function in photoactive and pharmacological activity.

Materials and methods

Materials

Pyromellitic dianhydride (96%), ethyl alcohol (96%), 1-ethyl (3-dimethylaminopropyl) carbodiimide hydrochloride (EDC) (93%), isopropanol (AR), o-phenylenediamine (99%) and sodium alginate (AR) were purchased from Shanghai Aladdin Biochemical Technology Co., Ltd.

Urea (AR), ferric chloride hexahydrate (AR), sodium hydroxide (99%), hydrochloric acid (GR), methanol (AR), tetrahydrofuran (AR), ammonium molybdate (AR), and sodium carboxymethyl cellulose (Degree of carboxymethylation, ≥80%) were purchased from Sinopharm Group Chemical Reagent Co. Ltd.

P-methoxy benzaldehyde (98%), vinyl acetate (98%), chloroacetic acid (98%), sodium dodecyl sulfate (95%), chitosan (Degree of deacetylation, ≥90%), and barium hydroxide (AR) were purchased from Shanghai Saan Chemical Technology Co. Ltd.

Preparation of biologically based photosensitive catalyzed active molecular capsule wall

Pyromellitic dianhydride (2.18 g), urea (15.03 g), and ferric chloride hexahydrate (1.35 g) were mixed in a mortar, then 2.36 g catalyst ammonium molybdate was added, fully ground. The resulting mixtures are heated at 180 °C for 0.5 h. After the reactant melted, the reaction was further heated at 230 °C for 5 h. The black part was soaked in 6 mol•L^{-1} hydrochloric acid for 12 h and then filtered. The filter cake was stirred in distilled water at 85 °C for 35 min and then filtered again. This stirring filtration was repeated until there was no solid precipitation of the filter solution. By drying the filtered residue, iron octadaminphthalocyanine (T) was obtained.

Sodium carboxymethyl cellulose (1.03 g) was dissolved in anhydrous ethanol (8.04 g). After 50 mL 20% sodium hydroxide solution was added and stirred for 0.5 h, iron octadaminphthalocyanine and 1-ethyl-(3-dimethyl aminopropyl) carbodiimide hydrochloric (EDC) were added to the resulting solution and stirred at 40 °C for 3.5 h, hot filtered, washed with 80% ethanol 5 times, and dried

at 100 °C for 4.5 h. In this way, the wall material (T- sodium carboxymethyl cellulose) were produced.

The capsule wall material of the alginic acid based photosensitive catalytic active molecular was the prepared in the same way as T-sodium carboxymethyl cellulose, and then obtained a new type of photosensitive catalytic active molecular capsule wall material (T-sodium alginate).

Chitosan (4.99 g) was dissolved in 50 mL 42% of NaOH solution, and stirred for 2 h in an ice bath to fully swell the chitosan. Isopropanol solution (25 mL) containing chloroacetic acid was added drop by drop. The resulting solution was stirred for 4 h at 0–15 °C; Then the pH was adjusted to 7.0, and the insoluble substance was removed by centrifuging. Appropriate amount of ethanol was added into the obtained supernatant, precipitating the product and allowed to stand for 2 h, then centrifuging, the product was washed with absolute ethyl alcohol 3 times, and vacuum drying to obtain the O-CMC. The obtained O-CMC was dissolved in distilled water. Then, sodium hydroxide solution was added, stirred for 0.5 h, and then iron octadaminphthalocyanine and 1-ethyl-(3-dimethylaminopropyl) carbodiimide hydrochloride (EDC) were added, heated and stirred for 3.5 h, filtered while hot, washed with 80% ethanol, and dried at 100 °C for 4.5 h, producing the photosensitive catalytic active molecular capsule wall material (T-carboxymethyl chitosan).

Preparation of algicide with a dual function in photoactive and pharmacological activity

The *p*-methoxy cinnamaldehyde was prepared as follows·THF solvent (20 mL), $Ba(OH)_2$ (3.6 g), vinyl acetate (1.03 g), and 4-methoxybenzaldehyde (1.36 g) were mixed in a three-necked round-bottom flask and refluxed for 10 h. Then the reactant was poured into ice water and filtered. The filtration was extracted with chloroform, then solvent was evaporated to give *p*-methoxy cinnamaldehyde.

The 2-aminobenzimidazole was prepared as follows. The mixture of O-phenylenediamine (1 mol) and 1 mol hydrochloric acid (30%) was heated to 90 °C. Then 1.2 mol cyanamide (45%) was added at a rate of 7 drops per min. After 40 min, 1.3 mol sodium hydroxide solution (35%) was added and continued to react for 40 min. The obtained product was suction-filtered, washed, and dried in vacuum for 12 h to give pale brown 2-aminobenzimidazole.

p-methoxy cinnamaldehyde (0.8 g) and 2-aminobenzimidazole (0.9 g) were dissolved in methanol (30 mL) and stirred for 1 h at 65 °C. The mixed solution was freeze-dried at −40 °C for 10 h to give the cinnamic aldehyde novel algae-killing compound (N-2-(4- methoxycyclohexyl-2,4-dienesubunits) ethylidene)-1-H-benzi midazole-2-amine).

Characterization of bio-based photosensitive catalytic active molecular materials and algicide agents

The absorption peak of the algae-killing compound was measured by an Ultraviolet spectrophotometer (UV-2550 UV, Shimadzu, Japan). The scanning wavelength was 200–900 nm. The IR spectra of iron octadaminphthalocyanine (T), T-CMC/SA/CMCS, and algae-killing compounds were determined by a Fourier transform infrared spectrometer (IRPrstige-21, Shimadzu, Japan) using the tableting method. The scanning wavelength was 400–4000 cm^{-1}. The ^1H NMR spectrum and ^{13}C NMR spectrum of iron octaphthalocyanine (T) were determined by Nuclear magnetic resonance spectrometer (Agilent 600 M, Agilent, USA). The conditions of ^1H NMR spectroscopy were as follows: data points were acquired 2048 times, scanning was done four times, the resonance frequency was 599.72 MHz, and adamantane was used as reference for the ^1H chemical shift. The ^{13}C NMR spectrum measurement conditions were as follows: data points were acquired 2048 times, scanning was done 3000 times, the resonance frequency was 150.72 MHz, and tetramethyl silane (TMS) was used as a reference for the ^{13}C chemical shift.

Preparation, characterization, and thermal stability of bio-based nanocapsules

All bio-based nanocapsules were prepared using a single polysaccharide

T-Carboxymethyl cellulose sodium (0.47 g) (or sodium alginate, carboxymethyl chitosan) was dissolved into distilled water (290 mL). Photoactive and pharmacological active double-efficacy algae-killing agent (N-2-(4-methoxycyclohexyl-2,4-diene subunits) ethylidene)-1-H-benzimidazole-2-amine) (0.37 g) was dissolved into toluene (28 mL), mixing the two phases evenly. Sodium dodecyl sulfate (2.5 g) was added, adjusting the pH to 5.6. This was stirred at high speed for 24 h, producing the sustained-release algae-killing nanocapsules.

The particle size of the algae-killing nanocapsules were measured by Zeta potential analysis (DT-300, Quantachrome, USA) at a temperature of 25 °C and a scattering angle of 90°. The morphology was observed by High-resolution transmission electron microscope (JEM-2100, Joel, Japan). The thermal decomposition temperature was measured by Differential scanning calorimeter (DSC Q2000, TA, USA). The temperature range was 20–200 °C, heated at a rate of 5 °C/min in a nitrogen atmosphere.

Determination of encapsulation efficiency of bio-based nanocapsules

Establishment of standard curves

High-performance liquid chromatographer (Agilent 1200, Agilent, USA) was used. The test conditions were as follows: a C_{18} reversed-phase chromatography column (Waters Company) was used in a mobile phase, with a methanol: water volume ratio of 3:2, flow rate of 0.8 mL·min^{-1}, detection wavelength of 319 nm; column temperature of 20 °C, and sample volume of 10 μL.

Algicide (0.1 g) was dissolved in the methanol–water solution (4:1, v/v) and diluted to 100 mL to obtain mother liquor of the algicide methanol–water solution (1 mg·ml^{-1}). The mother liquor was diluted to 0.06, 0.04, 0.02, 0.01, and 0.008 mg·mL^{-1}, shaken well, then passed through a 0.22-μm nylon membrane, and measured by HPLC, which was used to draw a standard curve.

Encapsulation rate determination

Sustained-release nanocapsules (3 mL, with a concentration of 1×10^4 mg·mL^{-1}) were centrifuged at 12,000 r·min^{-1} for 1 h. the supernatant (0.1 mL) was diluted to 10 mL with a methanol–water mixture (4:1, v/v), and then passed through a 0.22-μm nylon membrane. The content of the algae-killing compound in the supernatant was determined by HPLC.

Test of sustained-release performance of bio-based nanocapsules

Nanocapsules (0.5 g) were added to a dialysis bag and mixed with a methanol–water mixture (600 mL, 1:1, v/v). At 0.5, 1, 2, 4, 7, 11, 16, 24, 36, and 48 h, respectively, the mixture (1 mL) was taken and diluted to 25 mL with methanol–water mixture. The sample was passed through the 0.22-μm nylon membrane, and the concentration of the mixture was analyzed by high-performance liquid chromatography (HPLC). Methanol-water mixture (1 mL, 1:1, v/v) was added to the original solution to keep the volume of the release medium constant.

Determination of the phytotoxic of new algicide to T. Grandis green algae

The culturing was done according to the literature [24]. The green algae of *T. grandis* was cultured in an SE liquid/solid medium. The culture methods include the mixed culture, isolation and purification culture, and drug culture. The experimental operations are as follows:

Mixed culture of green algae: a proper amount of *T. grandis* green algae mixture was cultured in a triangular flask at 23 ± 2 °C with a light intensity of 6000 lx (120 μmol·m^{-2}·s^{-1}), continuously lit for 24 h per day over 2 weeks.

The culture of green algae was separated and purified as follows. The mixed culture of green algae was inoculated on an SE solid culture medium by plate scribing. After 1 week of continuous culturing, the green algae were inoculated into the SE liquid medium for the amplification culture.

The culture medium containing medicine was prepared as follows. First, an algicide solution was prepared in methanol with a concentration of 1000 mg·L^{-1}. The mother liquid (0.1 mL, 0.2 mL, 0.4 mL, 0.6 mL, and 1 mL) were then added to the green algae culture medium, with a concentration gradient of 0.05 mg·L^{-1}, 0.1 mg·L^{-1}, 0.2 mg·L^{-1}, 0.3 mg·L^{-1}, and 0.5 mg·L^{-1}. At the same time, a control group was set up and repeated three times. Sealed the Petri dish with preservative film and cultured in an incubator at a temperature of 28 °C. The color of the algae liquid was regularly observed during culturing by taking pictures.

Results and discussion

The synthesis of new biologically based materials and algae-killing compounds

The synthesis route of iron octadaminphthalocyanine(T), T-CMC (R_1), T-SA(R_2), and T-CMCS(R_3) was illustrated in Fig. S1. The iron octaaminophthalocyanine was prepared by solid melt tetrapolymerization. The carboxy group on the CMC, SA, and O-CMCS molecular chain reacted with the amino group of the iron octamethylphthalocyanine in the presence of EDC/NHS as activating agent. Thus, Iron octaaminophthalocyanine was grafted onto the molecular main chain of CMC, SA, and O-CMCS, and then produced T-CMC/SA/CMCS.

The synthesis route of the algae-killing compound is illustrated in Fig. S2. Cinnamaldehyde is often used in food spices because it kills bacteria and algae and does not cause pollution. The *p*-methoxy cinnamaldehyde was synthesized from p-methoxybenzaldehyde and vinyl acetate by a Prins addition reaction. 2-aminobenzimidazole was prepared by o-phenylenediamine and amino cyanide under acidic conditions, and (N-2-(4-methoxycyclohexyl-2,4-dienesubunits) ethylidene)-1 -H-benzimidazole-2-amine was obtained by imidization of *p*-methoxy cinnamaldehyde and 2-aminobenzimidazole.

The synthesized algicidal compound could be decomposed into two monomeric substances under the action of the alkaline plant cell liquid, achieving the expected control. The algicidal principle is shown in Fig. S3. As shown in Fig. S4, under the condition of a weak acid, the new biological matrix contains many –COO- groups with negative charge. The change in conformation of the molecular chain in the solution caused more –COO- to be exposed to the outside of the microcapsule, and the hydrophobic end of iron octadaminphthalocyanine (T) was taken as the inner layer of the capsule wall, thus encapsulating the new algicide inside. The resulting nanocapsules were collected and the yield of the product was calculated to be 72%.

Structure characterization of biological-based materials and algae-killing compounds

UV spectral analysis of cinnamaldehyde algae-killing compounds

Fig. 1 shows the UV spectrum analysis of cinnamaldehyde algae-killing compounds.

As shown in Fig. 1A, the maximum absorption wavelengths of 2-aminobenzimidazole and *p*-methoxy cinnamaldehyde were estimated by Woodward's rules:

$$\lambda_{\max} = \lambda_{basal} + \sum n_i \lambda_i$$

where $\lambda_{\max}$ is the maximum absorption wavelength of the compound, λ_{basal} is the base value of the compound matrix, and $n_i\lambda_i$ is the correction value for the number and type of substituents. The maximum absorption wavelength of 2-aminobenzimidazole and *p*-methoxy cinnamaldehyde was calculated according to the rules, both of which corresponded to the ones shown in the figure, indicating that 2-aminobenzimidazole and *p*-methoxy cinnamaldehyde were successfully synthesized.

Fig. 1B shows the UV spectra of the cinnamaldehyde algae-killing agent. Because this compound contains 9 conjugated double bonds, the maximum absorption wavelength was calculated according to the Fieser-Kuhn rule:

$$\lambda_{\max} = 114 + 5M + n(48 - 1.7n) - 16.5R_{endo} - 10R_{exo}$$

where n is the number of conjugated double bonds, M is the number of substituted alkyl groups and ring groups on the conjugated system, R_{endo} is the number of double bonds in the ring on the conjugated system, and R_{exo} is the number of double bonds outside the ring on the conjugated system. The calculated $\lambda_{\max}$ was 319.3 nm, and the error shown in the figure was within 10 nm. Thus, the cinnamaldehyde intelligent sustained-release algae-killing compound were successfully prepared.

Infrared spectrum of the bio-based molecular capsule wall materials

Fig. 2 shows an infrared spectrum analysis of the bio-based molecular capsule wall materials.

As shown in Fig. 2, iron octaaminophthalocyanine (Fig. 2e) shows a 1, 2, 4, 5-tetrasubstituted C-H out-of-plane vibration of the benzene ring near 855 cm^{-1}, and a medium-strong absorption peak of C = C and C = N near 1667 cm^{-1}. The absorption vibration peak appeared near 1142, 1161, and 1585 cm^{-1}, indicating the formation of the macrocyclic skeleton of phthalocyanine [25]. The C = O absorption peak of ketone compound appeared near 1715 cm^{-1}. The single-bond vibration of –NH_2 appeared near 750 cm^{-1}. It was tentatively inferring that iron octaaminophthalocyanine was synthesized.

The broad peak of carboxymethylcellulose sodium (CMC, Fig. 2a) near 3430 cm^{-1} corresponds to the O-H stretching vibration; the stretching vibration of C-H saturated single bond occurred near 2909 cm^{-1}. There was the carboxymethyl –CH_2 bending vibration and the C = O stretching vibration near 1595 cm^{-1}, and 1060 cm^{-1}; sodium alginate (SA, Fig. 2b) showed the O-H stretching vibration peak near 3600–3000 cm^{-1}, and the C = O stretching vibration of carboxyl group (–COOH) appeared near 1646 cm^{-1}; chitosan (CTS, Fig. 2c) showed a broad, strong absorption peak near 3425 cm^{-1}, which was the result of partial overlap of the characteristic absorption peaks of –OH and –NH_2. The in-plane bending vibration of –NH_2 appeared near 1650 cm^{-1}, and the vibration absorption peak of the alcoholic hydroxyl group appeared near 1100 cm^{-1}.

Compared with CTS (Fig. 2c), in addition to the vibration absorption peak of chitosan, O-CMCS (Fig. 2c_1) also showed a superposition peak of –COO- asymmetric stretching vibration

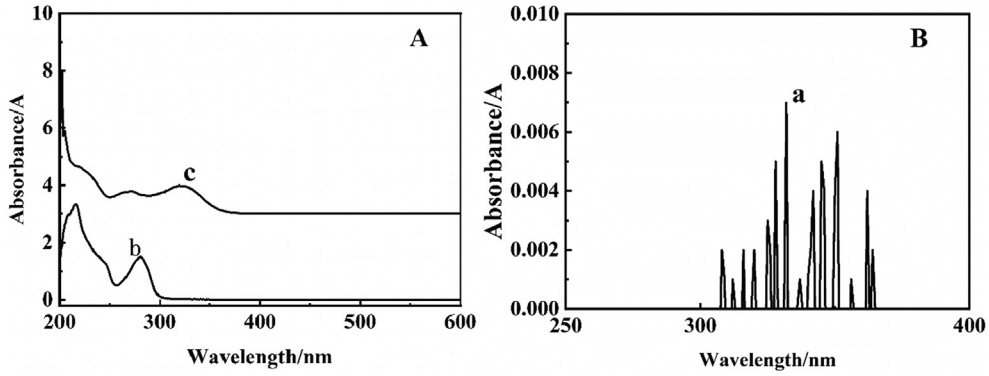

Fig. 1. UV absorption spectra of algicide (a), 2-aminobenzimidazole (b) and p-methoxy cinnamaldehyde (c).

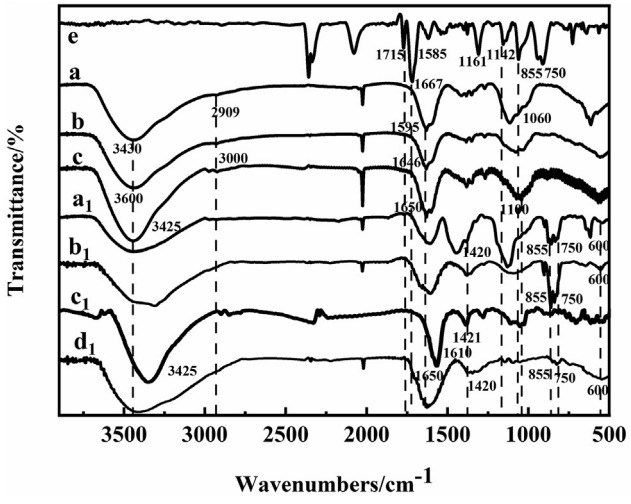

Fig. 2. FT-IR spectra of photosensitive materials and new biomass materials. a. CMC; b. SA; c. CTS; a_1. T-CMC; b_1. T-SA; c_1. O-CMCS; d_1. T-CMCS; e. Iron octaaminophthalocyanine.

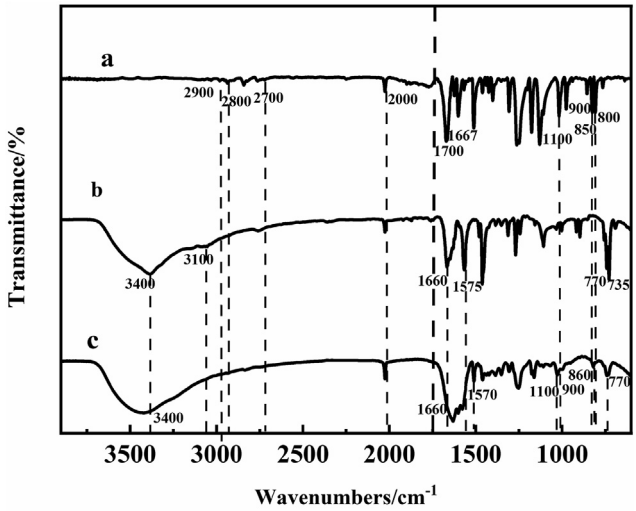

Fig. 3. FT-IR spectra of p-methoxy cinnamaldehyde (a), 2-aminobenzimidazole (b) and cinnamaldehyde algae killing compound (c).

and $-NH_2$ in-plane bending vibration near 1610 cm^{-1}. There was a symmetric stretching vibration peak of –COO- near 1421 cm^{-1}, and the alcohol hydroxyl absorption peak near 1100 cm^{-1} weakens, indicated that O-CMCS with carboxymethyl ($-CH_2$-O-COOH) structure had been successfully synthesized.

Compared with CMC (Fig. 2a), SA (Fig. 2b), and CTS (Fig. 2c), T-CMC (Fig. 2a_1), T-SA (Fig. 2b_1), and T-CMCS (Fig. 2d_1) show a new absorption peak at 750–600 cm^{-1}, which was the single bond vibration of $-NH_2$; The peaks at 870–855 cm^{-1} respond to benzene ring 1, 2, 4, 5-tetra substituted C-H out of plane vibration, The peaks at 1670–1420 cm^{-1}, respond to the superposition peaks of amide, C = C and C = N [26,27], indicating the presence of phthalocyanine skeleton. Therefore, it was inferred that photosensitive catalytic material most likely grafted to CMC, SA, O-CMCS molecular chain. These results show that T-CMC, T-SA, and T-CMCS were synthesized successfully.

Infrared spectroscopic analysis of cinnamaldehyde algae-killing compounds

The infrared spectrum analysis of cinnamaldehyde algae-killing compounds was shown in Fig. 3.

Fig. 3 shows that *p*-methoxy cinnamaldehyde (Fig. 3a) had multiple peaks at 2000–1667 cm^{-1} corresponding to benzene ring and peaks at 850–800 cm^{-1} corresponding to counterpoint double substitution of the benzene ring. The peak near 2700 cm^{-1} and 2800 cm^{-1} respond to C-H bond of the aldehyde structure. The peak near 1700 cm^{-1} respond to the C = O vibration absorption, indicating an aldehyde structure in *p*-methoxy cinnamaldehyde (Fig. 3a). A strong peak near 1100 cm^{-1} corresponds to C-O-C. A weak symmetrical absorption peak occurred near 900 cm^{-1}. The peaks at 3000–2900 cm^{-1} correspond to the C-H stretching vibration, which indicated that there was an $O-CH_3$ structure in *p*-methoxy cinnamaldehyde (Fig. 3a). 2-aminobenzimidazole (Fig. 3b) showed peak near 770–735 cm^{-1} which responds to the adjacent double substitution structure of the benzene ring; The peak near 1660–1575 cm^{-1} is attributed to -C = N. The double peaks near 3400–3100 cm^{-1} respond to $-NH_2$, which indicates the presence of imidazole group. Compared with the infrared spectra of *p*-methoxy cinnamaldehyde (Fig. 3a) and 2-aminobenzimidazole (Fig. 3b), the infrared absorption of cinnamaldehyde algae-killing compound (Fig. 3c) showed no peaks near 2800 cm^{-1} and 2700 cm^{-1}, and the double peaks at 3400–3100 cm^{-1} changed to a single peak, indicated that a cinnamaldehyde algicide was successfully synthesized.

Nuclear magnetic resonance spectroscopy analysis of iron octaaminphthalocyanine

The nuclear magnetic resonance spectra of iron octaaminphthalocyanine was shown in Fig. 4.

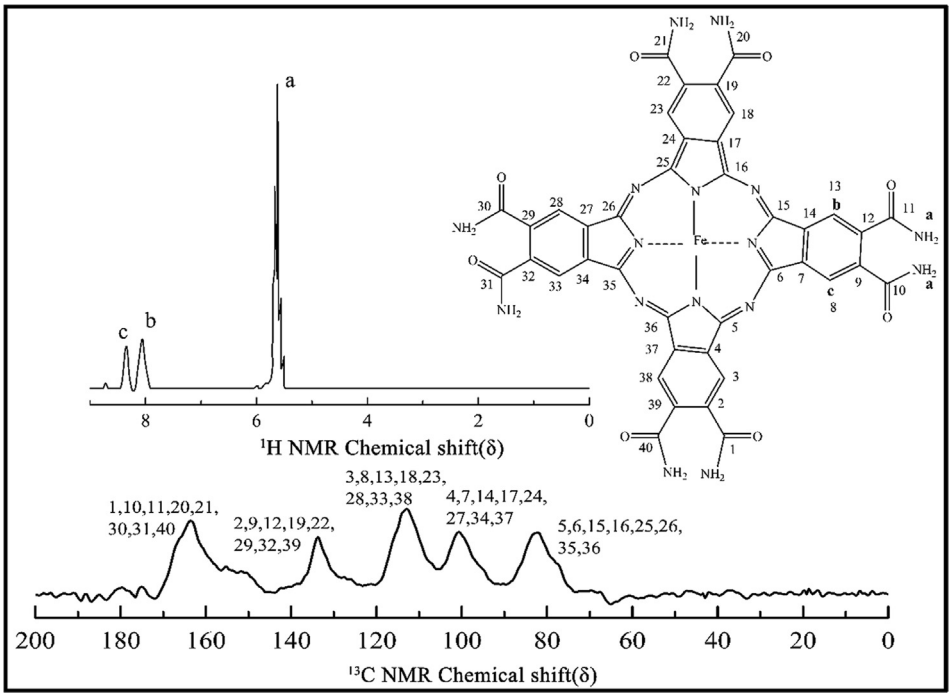

Fig. 4. ^{1}H NMR & ^{13}C NMR of iron octadaminphthalocyanine (T).

As shown in Fig. 4, the peak of δ = 5.5–5.7 ppm in ^{1}H NMR spectrum of iron octaaminophthalocyanine (T) was the chemical shift of –NH_2 connected to the framework of phthalocyanine iron. The peaks of δ = 7.9–8.1 ppm and δ = 8.3–8.5 ppm responds to the two kinds of *H* above the octaaminophthalocyanine ferrobenzene ring, respectively, and the peak area ratio was 4:1:1. Because of the electronegativity of the carbonyl group on the phthalocyanine skeleton and the intramolecular hydrogen bond, the *H* on the benzene ring moved to the low field (from δ = 7.3 ppm). The chemical shift of *H* on the *c* position was affected by the conjugation effect of the N = C double bond, and the electron cloud density was lower than that of the *b* position, so the peak appeared at the lower field. Because there was no hydrogen on the adjacent carbon of the three kinds of hydrogen, there was no split peak. These results show that iron octaaminophthalocyanine with a phthalocyanine iron skeleton was successfully synthesized [28,29].

The ^{13}C NMR spectrum of iron octaaminophthalocyanine was analyzed. The peak of *C1* (amide carbon atom) appeared at δ = 164 ppm, and the carbon skeleton nuclear magnetic spectrum peak of *C2*, *C3*, and *C4* appeared at δ = 134, 114, and 101 ppm, respectively. The chemical shifts of *C2*, *C3*, and *C4* decreased because the skeletal shielding effects of *C2*, *C3*, and *C4* were enhanced. The *C5* atom had the strongest skeleton shielding effect, so its deviation from the theoretical value was the greatest. The spectrum peak of the phthalocyanine skeleton appeared at δ = 83 ppm. These results show that the phthalocyanine skeleton was successfully prepared.

Morphology and thermal stability of drug-loaded capsules

Fig. 5 shows the particle-size and thermal analysis of the drug-loaded nanocapsules, and Fig. 6 shows TEM imagery.

Fig. 5 shows that the average particle size of the drug-loaded nanocapsules was 276 nm and larger than the blank particle size, the polydispersity coefficient (PDI) was 0.133, found by particle size measured by zeta potential analyzer (Fig. 5a), indicating that the particle size of the nanocapsules was relatively uniform. The thermal analysis diagram (Fig. 5b) shows that the decomposition temperature of the nanocapsules was above 40 °C, indicating good heat resistance. The particle size of the nanocapsules, as shown in Fig. 6, was about 10–30 nm, but the particle size measured by particle size measured by zeta potential analyzer was larger than that measured by transmission electron microscopy, mainly due to the partial aggregation of the nanocapsules in solution which increased the measured particle size. As shown in Figs. 5 and 6, the expected drug-loaded sustained-release nanocapsules were obtained.

Drug loading and release properties of biologically based nanocapsules

HPLC standard curve

The standard curve and HPLC of cinnamaldehyde algae-killing compound were shown in Fig. S5.

According to the HPLC of the cinnamaldehyde algicide standard (Fig. S5A) and the cinnamaldehyde algae-killing nanocapsules (Fig. S5B), the retention time of the cinnamaldehyde algicide was 12 min. a linear regression based on the peak spectrogram area for the mass concentration of the cinnamaldehyde algicide were performed, establishing the standard curve of HPLC. A regression equation with a good linear relationship was obtained: y = 29461*x* − 58.997 (*SD* = 654.1902, R^2 = 0.9914).

Entrapment efficiency of biologically based nanocapsules

Using Eq. (1), the encapsulation efficiency of the sustained-release nanocapsules θ was calculated:

$$\theta/\% = \frac{M_1 - m_1}{M_1} \times 100\% \quad (1)$$

Where in M_1 is the total algae-killing compound mass (mg) and m_1 is the mass of the algae-killing compound in the supernatant (mg). According to Eq. (1), the encapsulation efficiency of the capsule was 48.77%, and its drug-carrying performance was improved.

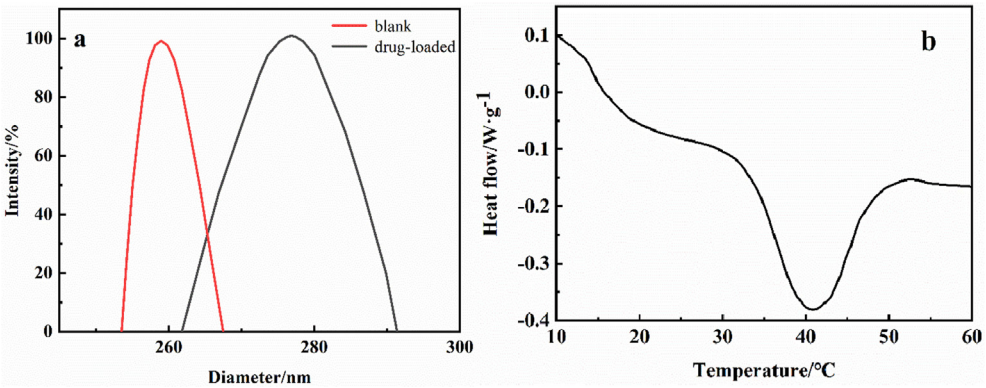

Fig. 5. Particle size (a) and thermal stability (b) of sustained-release nanocapsules.

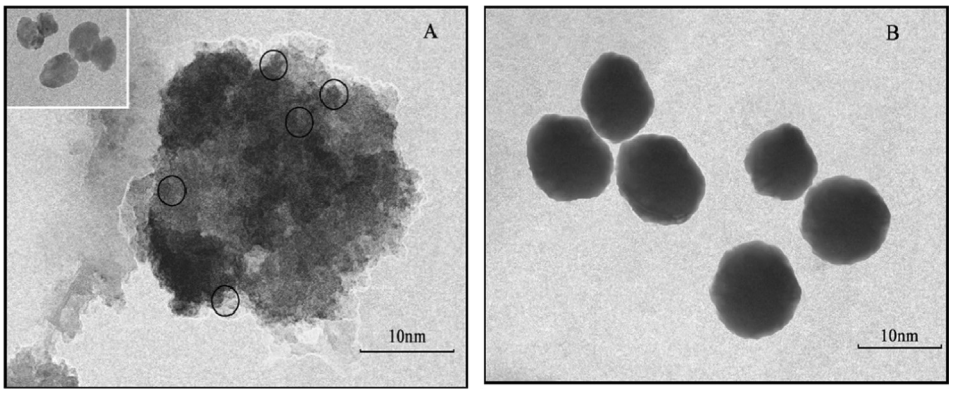

Fig. 6. TEM imagery (A/B) of sustained-release nanocapsules.

Sustained-release properties and release kinetics of drug-loaded nanocapsules

The release kinetics of the sustained-release behavior of drug-loaded nanocapsules was studied. The Peppas equation [30], Eq. (2), were used for fitting and obtained the model parameters shown in Table 1. The correlation of the drug release characteristic index n of the Peppas equation is found as:

$$\ln\frac{M_t}{M_\infty} = \ln K + n\ln t \quad (2)$$

Where M_t is the cumulative release at time t, M_∞ is the cumulative release at ∞, k and n are model parameters, and t is the release time.

When $n \leq 0.45$, the drug release mechanism is Fick diffusion, when $0.45 < n < 0.89$ it is non-Fick diffusion, and when $n \geq 0.89$ it is skeleton dissolution [31].

This model was suitable for data analysis at $t \leq 24$ h. As shown in Table 1, with a correlation coefficient of $r \geq 0.9$, the release of the nanocapsules agreed with the model equation: $n \leq 0.45$, so the drug release followed the Fick diffusion, mainly drug diffusion. The release mechanism was generally as follows: the nanocapsules which formed in the water were affected by changes in the environment such as the temperature and water flow. Water entered into the nanocapsules meanwhile the algae-killing compound was released from the nanocapsules so that reduced the stability of the drug-loaded nanocapsules.

Fig. 7 shows the cumulative drug release rate of the drug-loaded nano capsules and the dissolution rate of the algae-killing agent.

As shown in Fig. 7 (A), the nano capsules released during the initial phase, with the release of the algicide reaching 29–72%, and the dissolution rate of the algae-killing agent from capsules is shown as in Fig. 7 (B). This quick release had two main reasons. One reason is that during the initial stage of microcapsule release, there was a large concentration difference of the drug inside and outside the capsule wall, which aided the diffusion of the substance; The other reason is that the surface layer of the microcapsule may have had some of the drug adhered to it, and this drug was more likely to spread than the drug in the core [32]. After the quick release, the nanocapsules entered a slow release phase for 40–60 h, indicating good sustained release; the release rate of the algae-killing compound became slower and slower at this stage, and finally it stopped being released. The final cumulative release of the drug was 83%. Compared with spraying algicide directly into the environment, the sustained release capsules prepared in this study can help reduce the harm of sudden release of pesticides and prolong the efficacy period.

Table 1
Fitting results of drug delivery rate of nanocapsules.

Treated group	k	n	R
Cinnamaldehyde nanocapsules	42.49	0.26	0.93

Phytotoxic of cinnamaldehyde algicide

To obtain the phytotoxic of algae-killing compound to the *T. grandis* green algae, the algae with different concentrations of algae-killing compound were cultured, and the growth of the algae in a long-term culture was observed. Pictures were taken at the same time every day. Fig. 8 compares the growth of green algae on the first and ninth days.

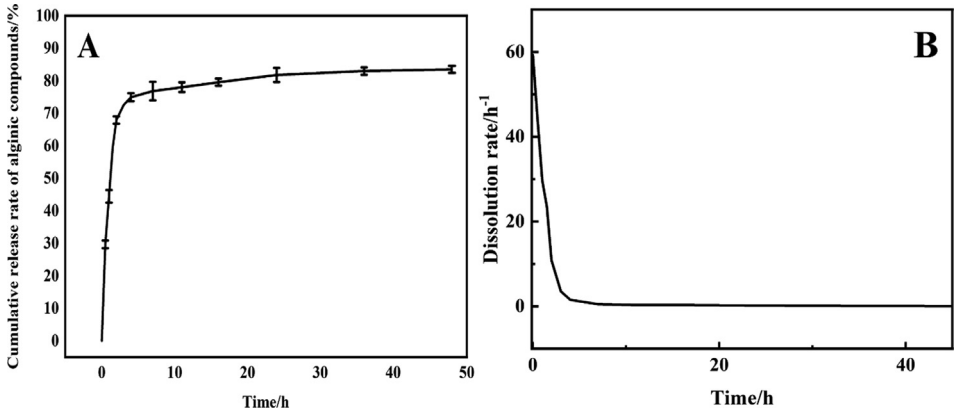

Fig. 7. Release profiles of drug-loaded nanocapsules.

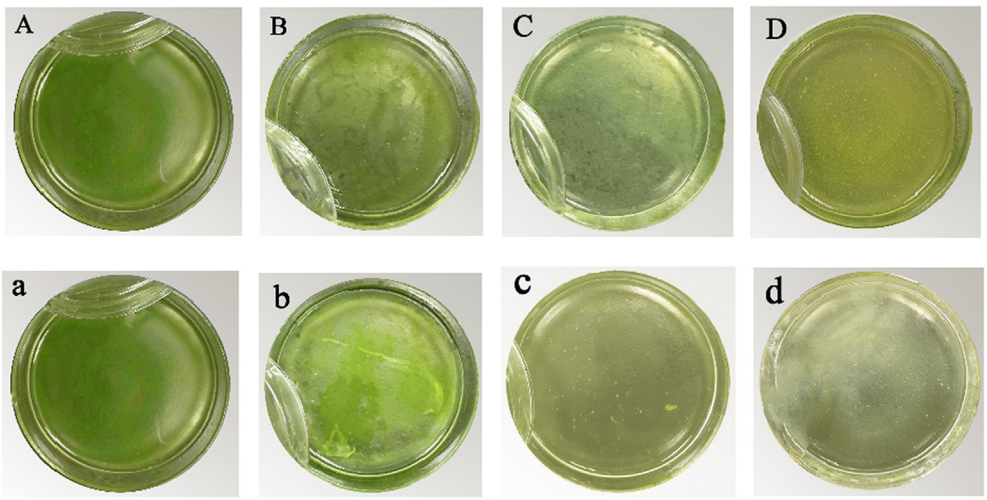

Fig. 8. The color change of green algae treated with algicide. (1 day (×mg·mL^{-1}) A: Control; B: 0.05; C: 0.2; D: 0.5; 9 days (×mg·mL^{-1}) a: Control; b: 0.05; c: 0.2; d: 0.5).

As shown above, on the ninth day, the 0.05 mg·mL^{-1} treatment barely affected the growth of the green algae; when the concentration reached 0.2 mg·mL^{-1}, the color of the green algae changed, indicating that the 0.2 mg·mL^{-1} concentration had an inhibitory effect; when the concentration reached 0.5 mg·mL^{-1}, the color of the green alga was close to yellow-white, indicated that the algicide at this concentration had killing effect on green algae.

The algae-killing compounds in this experiment are insoluble in water but dissolve in the organic solvent toluene. After culturing for some time, toluene volatilizes and the culture medium was left as a yellow suspension [33]. Because algae-killing compounds are difficult to dissolve in water and produce yellow precipitation, it is not perfect and rigorous to analyze the growth of green algae by only observing its color. It is more persuasive if we consider chlorophyll *a*, superoxide dismutase activity. However, this experiment can still provide a certain theoretical basis for the treatment of *T. grandis* green algae.

The results show that when the concentration of algae-killing compound was 0.2 mg·mL^{-1}, the growth of the green algae was inhibited, and when its concentration was 0.5 mg·mL^{-1}, the algae removal was obvious.

Conclusions

The bio-based molecular capsule wall was prepared by using carboxymethyl cellulose, chitosan and sodium alginate as raw materials, and using iron octaaminphthalocyanine as a modifier. The algae-killing compound was synthesized by using *p*-methoxy cinnamaldehyde and 2-aminobenzimidazole. The formed nanocapsules had a particle size of 10–30 nm, were stable below 40 °C, and showed good heat resistance. The encapsulation efficiency was 48.77%, and the final cumulative release rate of 60 h was 83%, indicating good drug loading and sustained release. This study also experimented with killing the algae of *T. grandis*. On the ninth day of the experiment, the algae-killing compounds at a concentration of 0.2 mg·mL^{-1} inhibited the green algae, and at a concentration of 0.5 mg·mL^{-1} they showed obvious inhibition and better control. Based on the structural analysis of the product and the qualitative and quantitative study of the nanocapsules, combined with the algae-killing experiments, the bio-based algae-killing nanocapsules were successfully prepared.

This study provides new encapsulating materials and algae-killing compounds for controlled-release pesticides. It also gives a new way to control *T. grandis* algae in an environmentally friendly way, which is important both in research and application.

Compliance with Ethics Requirements

This article does not contain any studies with human or animal subjects.

Declaration of Competing Interest

The authors declare that they have no known competing financial interests or personal relationships that could have appeared to influence the work reported in this paper.

Acknowledgements

This work was supported by the Scientific and Technological Cooperation Project of People's Government of Zhejiang Province-Chinese Academy of Forestry (2019SY09), and the Zhejiang Public Welfare Technology Application Research Project (LGN20B070001).

Appendix A. Supplementary data

Supplementary data to this article can be found online at https://doi.org/10.1016/j.jare.2020.12.006.

References

[1] Shi LK, Zheng L, Mao JH, Zhao CW, Huang JH, Liu RJ, et al. Effects of the variety and oil extraction method on the quality, fatty acid composition and antioxidant capacity of Torreya grandis kernel oils. Food Sci Technol 2018;91:398–405.
[2] Wang Y, Gao Z, Shen F, Li Y, Zhang S, Ren X, et al. Physicochemical Characteristics and Slow Release Performances of Chlorpyrifos Encapsulated by Poly (butyl acrylate-co-styrene) with the Cross-Linker Ethylene Glycol Dimethacrylate. J Agric Food Chem 2015;63:5196–204.
[3] Wu CB, Wu G, Yang X, Liu YJ, Gao CX, Ji QH, et al. Preparation of Mannitol @Silica core-shell capsules via an interfacial polymerization process from water-in-oil emulsion. Colloids Surf, A 2014;457:487–94.
[4] Song XQ, Duan YP, Li YX. Preparation of High Security N-Octadecane Micro PCMs by In Situ Polymerization. Appl Mech Mater 2015;727:141–4.
[5] Wang HC, Grolman JM, Rizvi A, Hisao GS, Rienstra CM, Zimmerman SC. pH-triggered release from polyamide microcapsules prepared by interfacial polymerization of a simple diester monomer. ACS Macro Lett 2017;6:321–5.
[6] Zuo M, Liu T, Han J, Tang Y, Yao F, Yuan Y, et al. Preparation and characterization of microcapsules containing ammonium persulfate as core by in situ polymerization. Chem Eng J 2014;249:27–33.
[7] Stark WJ, Stoessel PR, Wohlleben W, Hafner A. Industrial applications of nanoparticles. Chem Soc Rev 2015;44:5793–805.
[8] Nedovic V, Kalusevic A, Manojlovic V, Levic S, Bugarski B. An overview of encapsulation technologies for food applications. Procedia Food Sci 2011;1:1806–15.
[9] Kailasapathy K. Encapsulation technologies for functional foods and nutraceutical product development. CAB Rev 2009;4:1–19.
[10] Madene A, Jacquot M, Scher J, Desobry S. Flavour encapsulation and controlled release-a review. Int J Food Sci Technol 2006;41:1–21.
[11] Liu L, Wu F, Ju XJ, Rui X, Wei W, Catherine HN, et al. Preparation of monodisperse calcium alginate microcapsules via internal gelation in microfluidic-generated double emulsions. J Colloid Interface Sci 2013;404:85–90.
[12] Chun LX, Li DC, Peng YZ, Zhao LZ, Chong C, Feng Z, et al. Synthesis and characterization of stimuli-responsive poly(2-dimethylamino-ethylmethacrylate)-grafted chitosan microcapsule for controlled pyraclostrobin release. Int J Mol Sci 2018;19:854–67.
[13] Kumar S, Bhanjana G, Sharma A, Sidhu MC, Dilbaghi N. Synthesis, characterization and on field evaluation of pesticide loaded sodium alginate nanoparticles. Carbohydr Polym 2014;101:1061–7.
[14] Singh B, Sharma DK, Kumar R, Gupta A. Controlled release of thiram from neem-alginate-clay based delivery systems to manage environmental and health hazards. Appl. Clay Sci 2010;47:384–91.
[15] Li D, Liu B, Yang F, Wang X, Shen H, Wu D. Preparation of uniform starch microcapsules by premix membrane emulsion for controlled release of avermectin. Carbohydr Polym 2016;136:341–9.
[16] Campos EVR, De OJL, Fraceto LF, Singh B. Polysaccharides as safer release systems for agrochemicals. Agron Sustainable Dev 2015;35:47–66.
[17] Covis R, Ladaviere C, Desbrieres J, Marie E, Durand A. Synthesis of water-soluble and water-insoluble amphiphilic derivatives of dextran in organic medium. Carbohydr Polym 2013;95:360–5.
[18] Broderick E, Lyons H, Pembroke T, Byrne H, Murray B, Hall M. The characterisation of a novel, covalently modified, amphiphilic alginate derivative, which retains gelling and non-toxic properties. J Colloid Interface Sci 2006;298:154–61.
[19] Yinsong W, Lingrong L, Jian W, Zhang Q. Preparation and characterization of self-aggregated nanoparticles of cholesterol-modified O-carboxymethyl chitosan conjugates. Carbohydr Polym 2007;69:597–606.
[20] Li H, Yu Z, Wang S, Zhang L, Yang L. Protection of photoactivity of photosensitizers by amphiphilic polysaccharide micelles. Chin J Polym Sci 2014;32:1413–8.
[21] Bei YY, Yuan ZQ, Zhang L, Zhou XF, Chen WL, Xia P, et al. Novel self-assembled micelles based on palmitoyl-trimethyl-chitosan for efficient delivery of harmine to liver cancer. Expert Opin Drug Delivery 2014;11:843–54.
[22] Chang R, Yang J, Ge S, Zhao M, Liang C, Xiong L, et al. Synthesis and self-assembly of octenyl succinic anhydride modified short glucan chains based amphiphilic biopolymer: Micelles, ultrasmall micelles, vesicles, and lutein encapsulation/release. Food Hydrocolloids 2017;67:14–26.
[23] Liu K, Liu Y, Yao Y, Yuan H, Wang S, Wang Z, et al. Supramolecular Photosensitizers with Enhanced Antibacterial Efficiency. Angew Chem, Int Ed 2013;52(32):8285–9.
[24] Hong JW, Jeong J, Kim SH, Kim S, Yoon HS. Isolation of a Korean domestic microalga, chlamydomonas reinhardtii KNUA021, and Analysis of Its Biotechnological Potential. J Microbiol Biotechnol 2013;23:375–81.
[25] Shaabani A, Maleki MR, Maleki A, Rezayan AH. Microwave assisted synthesis of metal-free phthalocyanine and metallophthalocyanines. Dyes Pigm 2007;74:279–82.
[26] Pushpamalar V, Langford SJ, Ahmad M, Lim YY. Optimization of reaction conditions for preparing carboxymethyl cellulose from sago waste. Carbohydr Polym 2006;64:312–8.
[27] Qi H, Liebert T, Meister F, Heinze T. Homogenous carboxymethylation of cellulose in the NaOH/urea aqueous solution. React Funct Polym 2009;69:779–84.
[28] Jin LH, Yi RP, Nai SC. The characterization method of the isomers of tetra-substituted metal phthalocyanines by ^{1}H NMR. Chin J Struct Chem 2001;20:144–8.
[29] Arnold K, Balaban TS, Blom MN, Ehrler OT, Gilb S, Hamoe O, et al. Electron autodetachment from isolated nickel and copper phthalocyanine-tetrasulfonate tetraanions: isomer specific rates. J Phys Chem A 2003;107:794–803.
[30] Ritger PL, Peppas NA. A simple equation for description of solute release I. Fickian and non-fickian release from non-swellable devices in the form of slabs, spheres, cylinders or discs. J Controlled Release 1987;5:23–36.
[31] Mahboubeh M, Mohammad AT, Masoud L, Sanjay M. Drug release profile in core-shell nanofibrous structures: A study on Peppas equation and artificial neural network modeling. Comput Meth Prog Bio 2014;113:92–100.
[32] Zhai Y, Liu M, Wan M, Li Y, Zhang M, Zhai G. Preparation and characterization of puerarin-loaded lipid nanocapsules. J Nanosci Nanotechnol 2015;15:2643–9.
[33] Wang N, Wang K, Wang C. Comparison of different algicides on growth of microcystis aeruginosa and microcystin release, as well as its removal pathway in riverways. Front Environ Sci Eng 2017;11:19–26.

Jinyun LI (1995-, female), Graduate student Institution: Zhejiang A&F University Department: College of Engineering Research field: Bio-based Materials Address: Hangzhou, Zhejiang 311300, China Email: lijinyunzafu@sina.com

Ming GUO (1967-, male), PhD Title: Professor, Master Tutor Institution: Zhejiang A&F University Department: College of Science Research field: Forestry Engineering, Forestry Chemistry Address: Hangzhou, Zhejiang 311300, China Email: guoming@zafu.edu.cn. Member of the Chinese Chemical Society. Mainly engaged in the preparation of new biomaterials and their application. Presided over more than 20 major projects, published more than 160 scientific research papers, 16 authorized patents. **Published paper:** Guo M, Wang J, Wang CG, Strong PJ, Jiang PK, Ok YS, Wang HL. Carbon nanotube-grafted chitosan and its adsorption capacity for phenol in aqueous solution. The Science of the Total Environment, 2019, 682: 340-347.

Yiping WANG (1971-, male), PhD Title: Professor, Master Tutor Institution: Zhejiang A&F University Department: College of Forestry and Bio-technology Research field: Forest EntomologyAddress: Hangzhou, Zhejiang 311300, China Email: wyp@zafu.edu.cn. Member of Forest Insect Committee of China Forestry Society, presided over more than 10 major projects, published more than 40 scientific research papers, 3 authorized patents, 6 software copyrights. **Published paper:** Wang YP, Liu ZW, Chen XX. Eastern palaearctic cynipid inquilines-the genus ceroptres hartig, 1840 with descriptions of two new species (hymenoptera: cynipidae: cynipinae). Annals of American of the Entomological Society, 2012, 105: 377-385.

Bihuan YE (1989-, female), PhD Title: Research Associate Institution: Zhejiang Academy of Forestry Research field: Forest Protection Address: Hangzhou, Zhejiang 310023, China Email: 393938188@qq.com. Member of The Forest Protection Innovation Team. **Published paper:** Ye BH, Zhang YB, Shu JP, Wu H, Wang HJ. RNA-sequencing analysis of fungi-induced transcripts from the bamboo wireworm melanotus cribricollis (Coleoptera: Elateridae) larvae. PLos One, 2018, 13: e0191187. DOI:10.1371/journal.pone.0191187.

Youwu CHEN (1974-, male), Master Title: Research Professor Institution: Zhejiang Academy of Forestry Research field: Plant Cultivation Address: Hangzhou, Zhejiang 310023, China Email: youwu_chen@tom.com. Presided over more than 10 projects, published more than 30 scientific research papers. **Published paper:** Chen YW, Ye HL, Shen JJ, Zhu TJ. Investigation on insect pest and natural enemy of carya

illinoensis in Zhejiang Province. Journal of Zhejiang Forestry Science & Technology, 2015, 35: 54-59.

Xuejuan YANG (1988-, female), PhD Title: Lecturer Institution: Zhejiang A&F University Department: College of Science Research field: Chemistry of Forest Products Address: Hangzhou, Zhejiang 311300, China Email: yangxuejuan2008@126.com. Mainly engaged in the synthesis and structural properties of polymer materials, participated in 3 fund projects, published 8 scientific research papers. Undertake the teaching tasks of "Organic chemistry experiment" and other courses. **Published paper:** Yang XJ, Wang CP, Li SH, Huang K. Study on the synthesis of bio-based epoxy curing agent derived from myrcene and castor oil and the properties of the cured products. RSC Advances, 2017, 7: 238-247.